Src and cortactin promote lamellipodia protrusion and filopodia formation and stability in growth cones

Yingpei He[a], Yuan Ren[a], Bingbing Wu[a], Boris Decourt[a], Aih Cheun Lee[a], Aaron Taylor[b], and Daniel M. Suter[a,b]
[a]Department of Biological Sciences and [b]Bindley Bioscience Center, Purdue University, West Lafayette, IN 47907

ABSTRACT Src tyrosine kinases have been implicated in axonal growth and guidance; however, the underlying cellular mechanisms are not well understood. Specifically, it is unclear which aspects of actin organization and dynamics are regulated by Src in neuronal growth cones. Here, we investigated the function of Src2 and one of its substrates, cortactin, in lamellipodia and filopodia of *Aplysia* growth cones. We found that up-regulation of Src2 activation state or cortactin increased lamellipodial length, protrusion time, and actin network density, whereas down-regulation had opposite effects. Furthermore, Src2 or cortactin up-regulation increased filopodial density, length, and protrusion time, whereas down-regulation promoted lateral movements of filopodia. Fluorescent speckle microscopy revealed that rates of actin assembly and retrograde flow were not affected in either case. In summary, our results support a model in which Src and cortactin regulate growth cone motility by increasing actin network density and protrusion persistence of lamellipodia by controlling the state of actin-driven protrusion versus retraction. In addition, both proteins promote the formation and stability of actin bundles in filopodia.

INTRODUCTION

Axonal growth and guidance are fundamental to the development and regeneration of the nervous system. The growing axon is guided by the neuronal growth cone, which detects and transduces different types of extracellular cues into changes of cytoskeletal and membrane dynamics (Lowery and Van Vactor, 2009; Dent *et al.*, 2011; Tojima *et al.*, 2011; Vitriol and Zheng, 2012). The peripheral (P) domain of growth cones contains mainly F-actin structures and is separated from the microtubule- and organelle-rich central (C) domain by the transition (T) zone. The P domain is organized into alternating lamellipodia containing a branched F-actin network and filopodia with bundles of actin filaments (Lewis and Bridgman, 1992). The actin cytoskeleton is critical for growth cone motility, steering, and modulation of the rate of axonal elongation, whereas the microtubule cytoskeleton is essential for basic axonal extension, as well as for growth cone navigation (Letourneau and Ressler, 1984; Marsh and Letourneau, 1984; Sabry *et al.*, 1991; Suter *et al.*, 2004; Conde and Caceres, 2009; Dent *et al.*, 2011; Gomez and Letourneau, 2014). Although many second messenger systems that regulate actin- and microtubule-binding proteins in neuronal growth cones have been identified (Bashaw and Klein, 2010; Dent *et al.*, 2011; Gomez and Letourneau, 2014; Sutherland *et al.*, 2014), the precise effects of these signaling pathways on cytoskeleton function are often unclear, since quantitative analysis of cytoskeletal dynamics at high temporal and spatial resolution is challenging in most growth cone model systems. To address this issue in the present study, we used the large *Aplysia* growth cones (Suter, 2011).

Src family tyrosine kinases regulate various biological processes, including cell proliferation, adhesion, migration, differentiation, and survival (Thomas and Brugge, 1997; Martin, 2001; Parsons and Parsons, 2004). In the nervous system, Src has been identified downstream of several attractive and repulsive guidance cues,

including immunoglobulin superfamily cell adhesion molecules (Ignelzi et al., 1994; Suter and Forscher, 2001), netrin-1 (Li et al., 2004; Liu et al., 2004; Robles et al., 2005), sonic hedgehog (Yam et al., 2009), ephrinA5 (Knoll and Drescher, 2004; Wong et al., 2004), and semaphorin 3B (Falk et al., 2005). Activation or inhibition of Src affects axonal or dendritic growth and guidance in a number of in vivo systems, including mouse cerebellar Purkinje cells (Kotani et al., 2007) and chick and mouse spinal motor neurons during limb trajectory selection (Kao et al., 2009), as well as in several identified neurons in Caenorhabditis elegans (Itoh et al., 2005). In vitro, global inhibition of Src blocks Aplysia cell adhesion molecule–evoked growth cone advance (Suter and Forscher, 2001), whereas asymmetric inhibition of Src induces repulsive turning of embryonic Xenopus growth cones (Robles et al., 2005). These findings demonstrate an important role of Src in axonal growth and guidance and raise the key question of how cytoskeletal organization and dynamics are regulated by Src in lamellipodia and filopodia, since the cytoskeleton is a major driving force of growth cone motility.

The Src-substrate and actin-binding protein cortactin is an important linker between Src signaling and the actin cytoskeleton. Besides directly binding to actin filaments, cortactin also interacts with the actin-related protein-2/3 (Arp2/3) complex and facilitates its actin-nucleating activity either directly or indirectly via neuronal Wiskott–Aldrich syndrome protein (N-WASP; Uruno et al., 2001; Weaver et al., 2001; Kowalski et al., 2005). Similar to Src, cortactin is involved in multiple cellular processes, such as cell adhesion, migration, and endocytosis (Ammer and Weed, 2008). In neuronal growth cones, cortactin localizes to both filopodia and lamellipodia (Korobova and Svitkina, 2008; Decourt et al., 2009; Kurklinsky et al., 2011; Yamada et al., 2013). However, very little is known about cortactin function in neuronal growth cones. A recent study suggests that cortactin stabilizes actin bundles by forming a ring-like structure together with dynamin 1 in growth cones (Yamada et al., 2013). Furthermore, cortactin facilitates formation of axonal filopodia and neurite branching (Mingorance-Le Meur and O'Connor, 2009; Spillane et al., 2012). The detailed functions of cortactin in filopodia and lamellipodia remain unclear, since both increasing and reducing cortactin expression resulted in enlarged growth cones (Cheng et al., 2000; Kurklinsky et al., 2011).

To achieve a more comprehensive understanding of how Src and cortactin control actin organization and dynamics in growth cone lamellipodia and filopodia, we used a range of imaging techniques, including high-resolution differential interference contrast (DIC) time-lapse imaging, actin fluorescent speckle microscopy (FSM), stochastic optical reconstruction microscopy (STORM), and scanning electron microscopy (SEM). We used these techniques to image Aplysia growth cones in different states of Src2 activation and cortactin protein levels under well-defined conditions and independent of any upstream stimuli. Our results support a model in which Src2, via phosphorylation of cortactin, promotes the protrusion of lamellipodia, as well as the formation, stability, and elongation of filopodia. Our findings suggest that these functions are likely mediated by increasing branch formation of actin filaments in lamellipodia, stabilizing actin bundles in filopodia, and by increasing the persistence of actin-driven protrusion rather than the rate of the actin assembly process.

RESULTS

Up- and down-regulation of Src2 and cortactin in neuronal growth cones

We previously identified the Aplysia Src tyrosine kinase Src2 as well as the Src substrate cortactin and characterized their localization in neuronal growth cones (Wu et al., 2008; Decourt et al., 2009). To investigate the mechanisms of how Src2 and cortactin control growth cone morphology and motility, we experimentally altered Src2 and cortactin protein levels and activation states in cultured Aplysia bag cell neurons by expressing various Src2 and cortactin constructs in a controlled manner. We chose this approach because Src and cortactin construct expression increased protein levels on average by 50–120% (Supplemental Figure S1), which is very modest compared with typical overexpression conditions after DNA plasmid transfections. Thus, the observed phenotypic changes were unlikely caused by overexpression artifacts. Furthermore, RNA interference knockdown approaches did not strongly reduce protein levels within a time frame that was optimal for analysis of actin dynamics after microinjections.

To up-regulate Src2 activation state, we expressed constitutively active Src2 (CASrc2), since expression of wild-type Src2 had relatively modest effect on growth cone morphology and motility, which is consistent with our previous study (Wu et al., 2008). To down-regulate Src2 activation state, we expressed either dominant negative Src2 (DNSrc2) or membrane localization–defective Src2 (MD-Src2). Untagged constructs were used in this study to avoid any potential effects of fluorescent proteins on localization, regulation, or activity of either Src2 or cortactin. We validated our expression approach by immunolabeling with antibodies against Src2, activated Src2 (pSrc2), and cortactin 2 d after microinjection, immediately after time-lapse imaging (Supplemental Figure S1). Because all neurons were coinjected with Alexa 568 G-actin to monitor actin dynamics, actin-only injections represented our control group. The reduction in Src2 activation after MDSrc2 expression is consistent with the observation that plasma membrane association is required for full activation of Src (Bagrodia et al., 1993) as well as with our previous results (Wu et al., 2008). Because MDSrc2 expression reduced levels of activated Src2 compared with controls (Supplemental Figure S1B) and had more significant phenotypic effects than DNSrc2 expression (Supplemental Figure S2), we focused on MD-Src2 expression as our main approach to down-regulate Src2.

To up-regulate cortactin levels, we expressed full-length Aplysia cortactin (Decourt et al., 2009). To investigate the function of cortactin phosphorylation in growth cones, we made a dominant negative construct of cortactin in which all three putative Src tyrosine phosphorylation sites were mutated (cortactin triple tyrosine phosphorylation mutant [Y499F-Y505F-Y509F]). Overexpression of both wild-type cortactin and CortF resulted in increased total cortactin levels in growth cones, and neither of them affected Src2 activation states, suggesting that cortactin does not regulate Src2 activation as expected (Supplemental Figure S1, C and D).

Src2 and cortactin promote persistent protrusions of lamellipodia

Src and cortactin were previously implicated in lamellipodial protrusion and migration of cancer cells (Bryce et al., 2005; Mezi et al., 2012). Here, we tested whether they function similarly in neuronal growth cones. DIC live-cell imaging revealed that CASrc2 and cortactin expression resulted in growth cones with lamellipodia that were on average 48 and 25% longer, respectively, than control growth cones (Figure 1, A, B, D, and F). Conversely, the lamellipodial lengths of MDSrc2- and CortF-expressing growth cones were reduced by 34 and 23%, respectively (Figure 1, A, C, E, and F). To confirm the role of Src2 in regulating lamellipodia, we treated growth cones with the Src family kinase inhibitor PP2 for 15 min. We found that pharmacological Src inhibition also reduced lamellipodial length, on average by 46% (Supplemental Figure S3). These
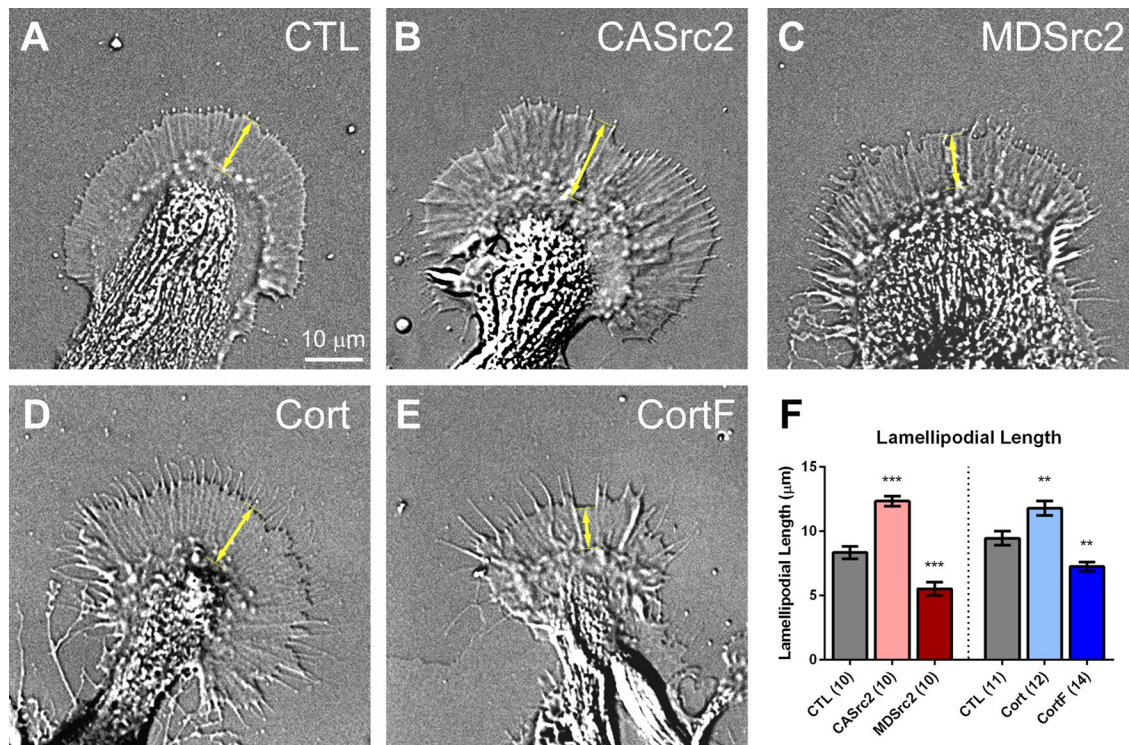
FIGURE 1: Src2 and cortactin increase the length of lamellipodia. (A–E) DIC live-cell images of *Aplysia* growth cones in control condition (CTL; A) and expressing CASrc2 (B), MDSrc2 (C), cortactin (D), or CortF (E). (F) Quantification of lamellipodial length, measured as the distance between the T zone and the leading edge (double-headed arrow in A–E). Mean values ± SEM. Numbers in parentheses are number of growth cones selected from at least three experiments. One-way ANOVA with Dunnett's post hoc test separately performed for Src2 and cortactin groups; $**p < 0.01$, $***p < 0.001$. Scale bar as indicated.

results show that Src2 and cortactin control the length of growth cone lamellipodia. In a previous study, we reported that CASrc2 expression decreased total growth cone size (Wu *et al.*, 2008). To better compare these earlier results with the present data, we also analyzed total growth cone size in the present study. Although not reaching a statistically significant level as in the case of lamellipodial length, CASrc2- or cortactin-expressing growth cones are larger than controls (unpublished data). Growth cone size is likely controlled by more pathways than lamellipodial length; thus we focused on length measurements here. The discrepancy between the previous and the present study in growth cone size effects after CASrc2 expression may arise from the difference in control conditions, the selection of growth cones, or both. In our earlier study, enhanced green fluorescent protein (EGFP)–expressing neurons served as the control condition, whereas actin-only injected cells represented our control group in the present study. EGFP-expressing cells were not included in the present analysis because EGFP expression can also affect endogenous Src2-levels (unpublished data). Furthermore, we quantified a wider range of growth cone morphologies without knowing the level of Src2 overexpression in the previous study, whereas in the present study, we only analyzed growth cones that showed a clear P domain and a minimum of 50% Src2 overexpression over control. In conclusion, we believe that the present CASrc2 data set better represents the effects of Src2 activation on lamellipodial length and size.

To determine which aspects of lamellipodial dynamics are regulated by Src2 and cortactin, we performed DIC time-lapse imaging on poly-L-lysine substrate on which growth cones translocate, albeit at a slow rate (Figure 2A). The leading edge of control growth cones growing on poly-L-lysine was frequently observed in the pausing phase (Figure 2A and Supplemental Video S1). CASrc2- and cortactin-expressing growth cones spent more time in the protrusion phase than did controls (Figure 2A and Supplemental Videos S2 and S4). MDSrc2- and CortF-expressing growth cones, on the other hand, exhibited a more dynamic leading edge behavior, with frequent switching between protrusion and retraction (Figure 2A and Supplemental Videos S3 and S5). Quantification revealed that control growth cones spent 57% of the time pausing, 25% protruding, and 18% retracting, whereas CASrc2-expressing growth cones spent significantly more time in protrusion (38%), less time in retraction (10%), and switched less frequently into retraction phases than did control (Figure 2, B', C, and C', and Supplemental Video S2). Down-regulating Src2 by expressing MDSrc2 increased the initiation frequency of protrusion and retraction phases by 38 and 56%, respectively, as well as retraction time by 40% (Figure 2, B, B', and C'). These results were confirmed by treating neurons with 25 µM PP2 for 15 min, which resulted in frequent switching between leading-edge retraction and protrusion (Supplemental Figure S3, A–D).

Cortactin up-regulation affected lamellipodial dynamics in a similar way as CASrc2 expression. We observed a 60% increase in protrusion time in cortactin-expressing growth cones (Figure 2C). CortF-expressing growth cones had an 88% increase in retraction time, as well as a 30% increase in retraction frequency (Figure 2, B' and C'), thus showing a similar phenotype as MDSrc2-expressing growth cones. Of importance, lamellipodial protrusion and retraction rates were not significantly influenced by any of the Src2 or cortactin constructs (rates were around 2 µm/min; Figure 2, D and D'); therefore, we conclude that Src2 and cortactin promote
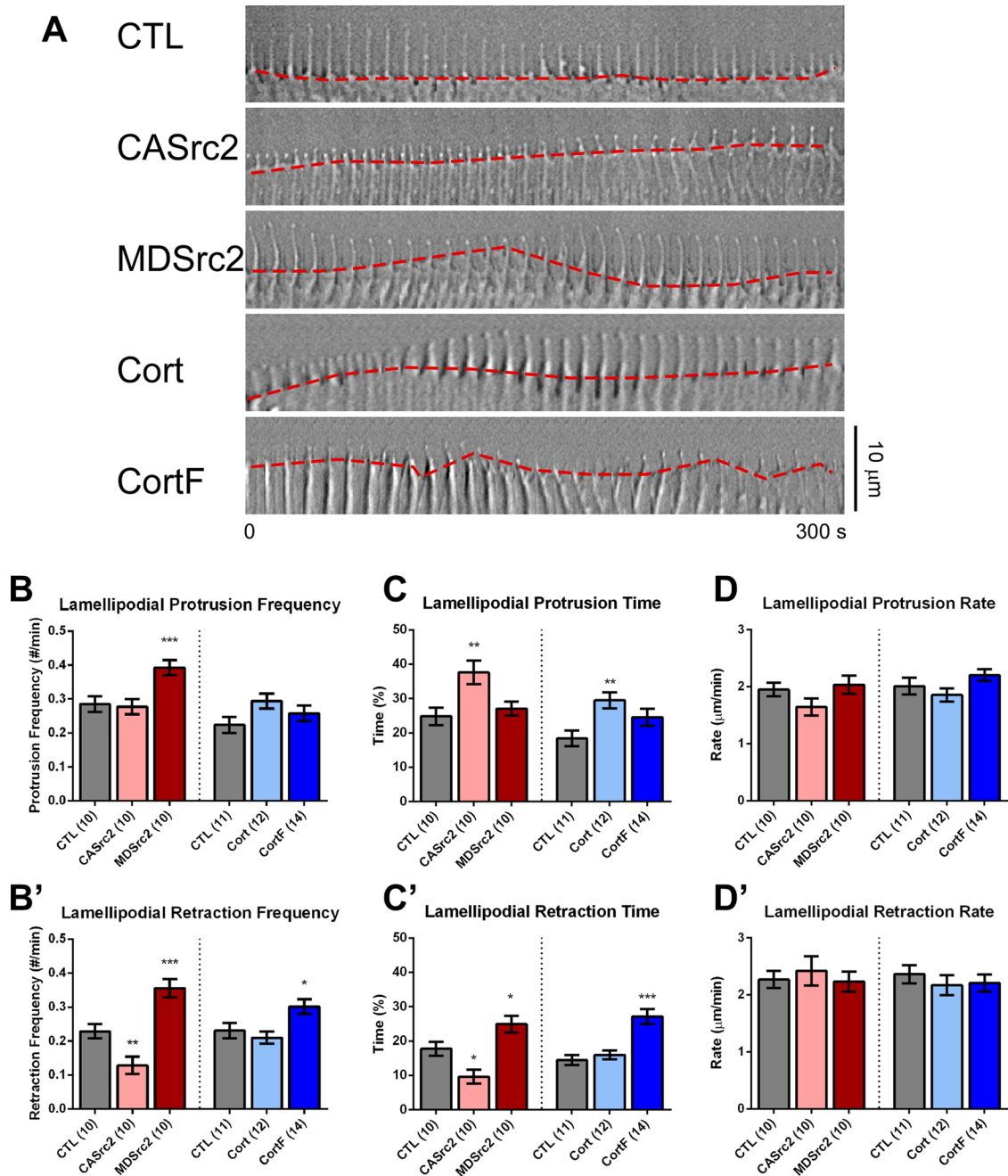
FIGURE 2: Src2 and cortactin positively regulate lamellipodial protrusion persistence. (A) DIC montages of 5-min time-lapse recordings at 10-s intervals showing lamellipodial leading-edge dynamics (red dashed line) in control growth cones or after expression of CASrc2, MDSrc2, cortactin, or CortF. Scale bar as indicated. (B, B') Respective protrusion and retraction frequencies of lamellipodia. (C, C') Respective average percentages of time lamellipodia spent in protrusion and retraction phases. (D, D') Respective average lamellipodial protrusion and retraction rates. Mean values ± SEM. Numbers in parentheses are number of growth cones selected from at least three experiments. One-way ANOVA with Dunnett's post hoc test was separately performed for Src2 and cortactin conditions; $*p < 0.05$, $**p < 0.01$, $***p < 0.001$.

protrusion of growth cone lamellipodia by increasing the persistence but not the rate of protrusion.

Src2 and cortactin positively regulate the density and stability of filopodia

Next we investigated whether and how Src2 and cortactin regulate filopodial morphology and dynamics. In control growth cones, we measured an average density of 0.8 filopodia/μm of leading edge (Figure 3, A and H). Expression of CASrc2 and cortactin increased the density of filopodia by 18 and 19%, respectively, whereas expression of CortF reduced density by 26% (Figure 3, B–E and H). Furthermore, Src2 and cortactin affected filopodial morphology and behavior. The majority of all filopodia (57%) in control growth cones were straight, perpendicular to the leading edge, and underwent
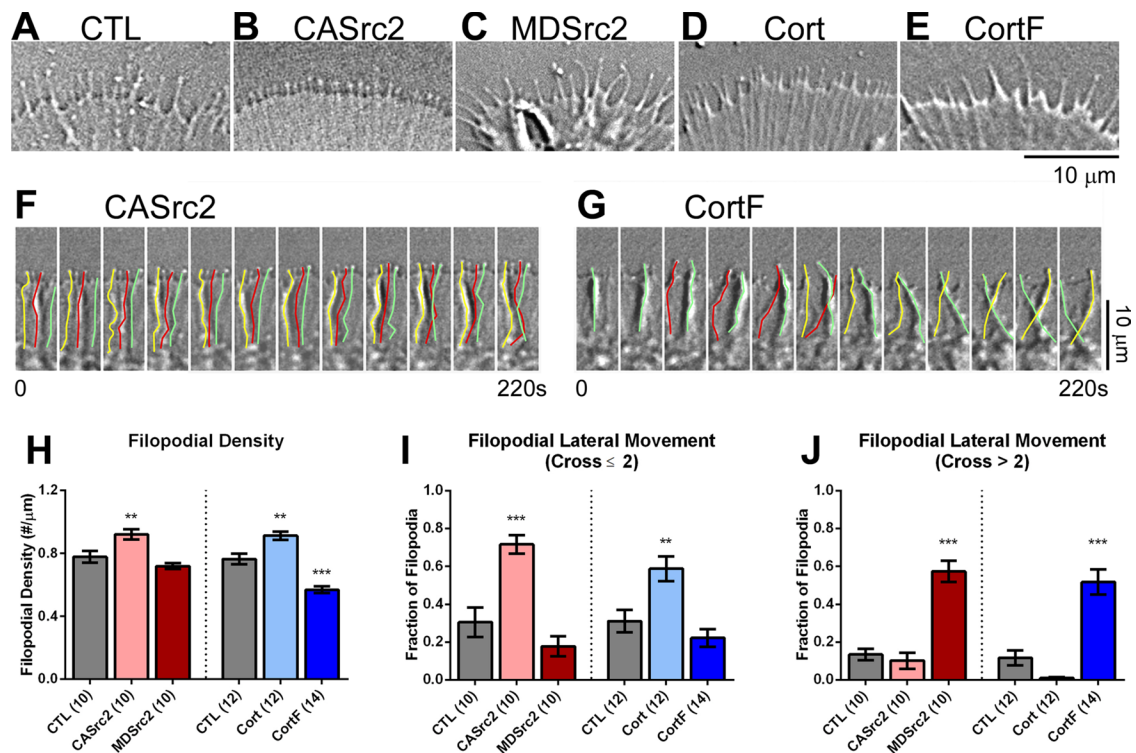
FIGURE 3: Src2 and cortactin regulate filopodial density and stability. (A–E) DIC images depicting the P domain of control (A) and CASrc2- (B), MDSrc2- (C), cortactin- (D), and CortF-expressing (E) growth cones. (F, G) DIC montages of a region of interest in the periphery of CASrc2- and CortF-expressing growth cones showing small-scale (F) and large-scale (G) lateral movements of filopodia traced with yellow, red, and green lines. Time interval between each image is 20 s; total time, 220 s. Scale bars as indicated. (H–J) Quantifications of filopodial density (H) along growth cone perimeter, as well as small-scale (I) and large-scale (J) filopodial lateral movements, respectively. Small-scale lateral movements were defined as filopodia that moved sideways no further than two adjacent filopodia. Large-scale lateral movements were defined as filopodia that moved sideways further than two adjacent filopodia. Mean values ± SEM; numbers are numbers of growth cones selected from at least three experiments. One-way ANOVA with Dunnett's post hoc test was separately performed for Src2 and cortactin conditions; **$p < 0.01$, ***$p < 0.001$.

few lateral movements. CASrc2 and cortactin expression increased the percentage of filopodia undergoing small-scale lateral movements (crossing fewer than two adjacent filopodia) by 135 and 89%, respectively (Figure 3, F and I), whereas MDSrc2 and CortF expression increased the percentage of filopodia undergoing large-scale lateral movements (crossing two or more adjacent filopodia) by 327 and 345%, respectively (Figure 3, G and J, and Supplemental Videos S1–S5). Furthermore, Src inhibition by PP2 significantly increased large-scale lateral movements of filopodia by 368% (Supplemental Figure S3F). Collectively these results suggest that Src2 and cortactin contribute to the formation of filopodia and have a significant role in the integration/stabilization of filopodia within the lamellipodial actin network.
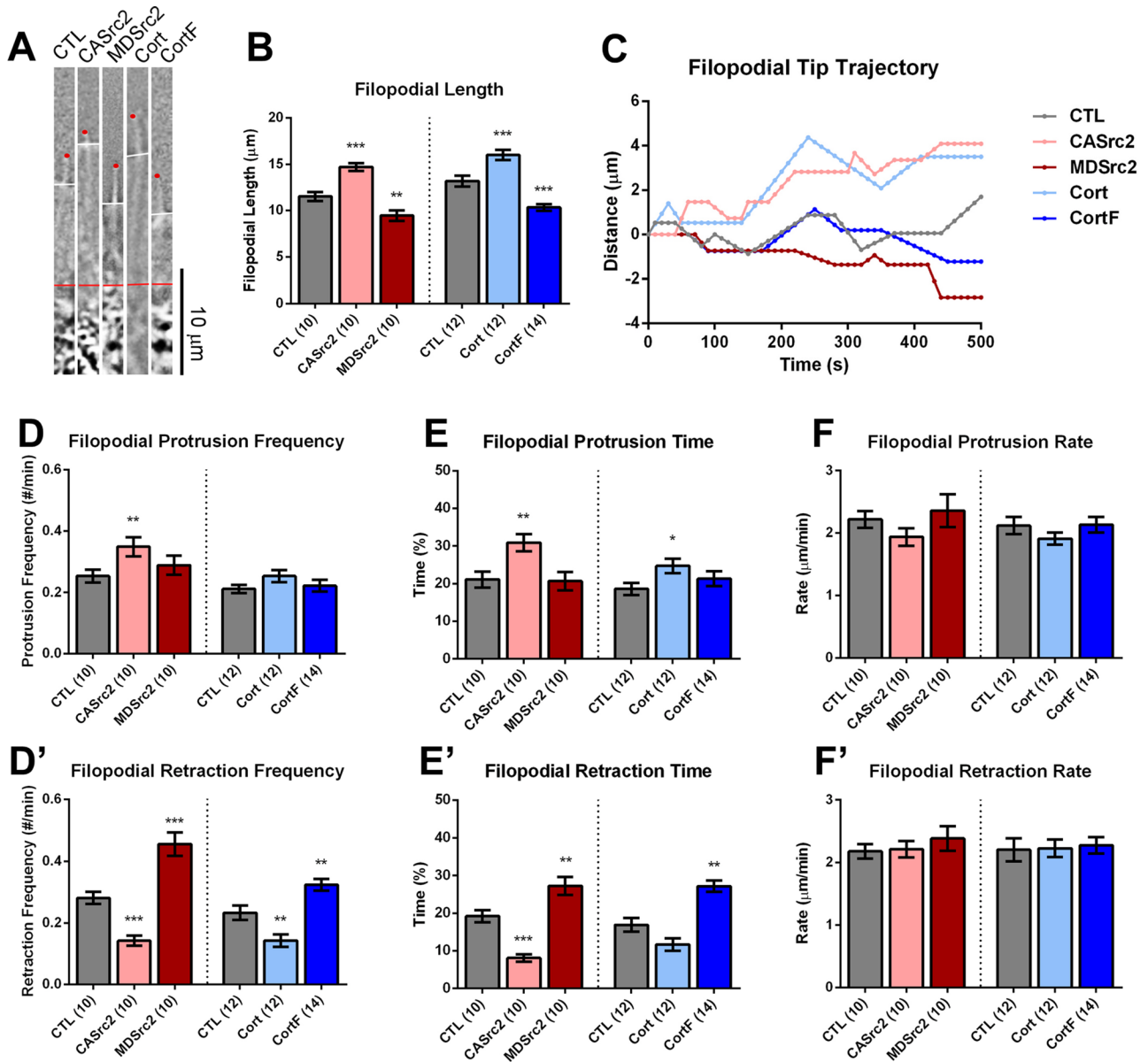
Src2 and cortactin facilitate elongation of filopodia
Previous studies suggested that Src and cortactin promote filopodial elongation in growth cones (Robles *et al.*, 2005; Wu *et al.*, 2008; Yamada *et al.*, 2013). Consistent with these findings, we measured the length of filopodia between the transition zone (T zone) and the filopodial tips and found that up-regulation of Src2 and cortactin increased filopodial length, whereas down-regulation had the opposite effect (Figure 4, A and B). We used time-lapse imaging to track the dynamics of individual filopodial tips and to determine which aspects of filopodial motility were affected by Src2 and cortactin expression (Figure 4, C–F′). We found that CASrc2 and cortactin

expression increased protrusion time by 46 and 33% and reduced retraction time by 58 and 31%, respectively, whereas MDSrc2 and CortF expression increased filopodial retraction time by 42 and 61%, respectively (Figure 4, E and E′). Furthermore, CASrc2 and cortactin expression reduced the frequency with which filopodia switched into retraction, whereas expression of MDSrc2 and CortF had the opposite effect (Figure 4D′). Similar to lamellipodia, the rates of filopodial protrusion and retraction were relatively constant, with values of ~2 μm/min under all conditions. These results suggest that Src2 and cortactin contribute to the length of filopodia by increasing protrusion persistence but not by controlling the rate of protrusion.

Cortactin acts downstream of Src2
Because CASrc2 and cortactin expression had similar effects that were opposite to the ones caused by MDSrc2 and CortF expression, we speculated that Src2-mediated cortactin phosphorylation controls actin organization and dynamics in growth cone lamellipodia and filopodia. To test this hypothesis, we coexpressed CortF together with CASrc2 to determine whether expressing the tyrosine phosphorylation–deficient mutant of cortactin diminishes the phenotype observed after increasing Src2 activation (Figure 5). We found that coexpression of CortF restored the phenotypes caused by CASrc2 expression to control levels, including the increase in lamellipodial length (Figure 5B), filopodial length (Figure 5C), filopodial density (Figure 5D), and small-scale filopodial lateral movements

FIGURE 4: Src2 and cortactin facilitate protrusion of filopodia. (A) One representative filopodium is shown for each experimental condition. Filopodial length was measured from the T zone (red line) to tip of the filopodium (red dot). The position of leading edge is marked with a white line. Scale bar as indicated. (B) Quantification of average filopodial length after Src2 and cortactin up- and down-regulation, respectively. (C) Distance vs. time plots of five representative filopodial tips for each experimental condition. (D, D') Filopodial protrusion and retraction frequencies were determined as the frequency of entering into protrusion and retraction phase, respectively, from any other phases. (E, E') Percentage of time filopodia spent in protrusion or retraction phase, respectively. (F, F') Filopodial protrusion and retraction rates, respectively. Mean values ± SEM; numbers in parentheses are number of growth cones selected from at least three experiments; one-way ANOVA with Dunnett's post hoc test was separately performed for Src2 and cortactin conditions; *$p < 0.05$, **$p < 0.01$, ***$p < 0.001$.

(Figure 5E). These data suggest that a significant fraction of Src2 effects on lamellipodia and filopodia is mediated by phosphorylated cortactin. Of interest, coexpression of CortF and CASrc2 also restored the large-scale lateral movement of filopodia caused by CortF expression to control levels (Figure 5F), suggesting that phosphorylated cortactin is critical for filopodial stability. In a similar vein, analysis of lamellipodial and filopodial dynamics revealed that coexpressing CortF reduced the positive effects of CASrc2 expression on protrusion time, as well as its negative effects on retraction time and frequency (Supplemental Figure S4). In summary, these results suggest that Src2 acts upstream of cortactin in a phosphorylation-dependent manner, playing an important role in controlling actin organization and dynamics in lamellipodia and filopodia of growth cones, specifically by enhancing the persistence of protrusions, as well as increasing the formation and stability of filopodial actin bundles.

The rates of actin assembly and retrograde flow are not controlled by Src2 and cortactin
Because the actin cytoskeleton is a major effector controlling morphology and motility of growth cone lamellipodia and filopodia, we
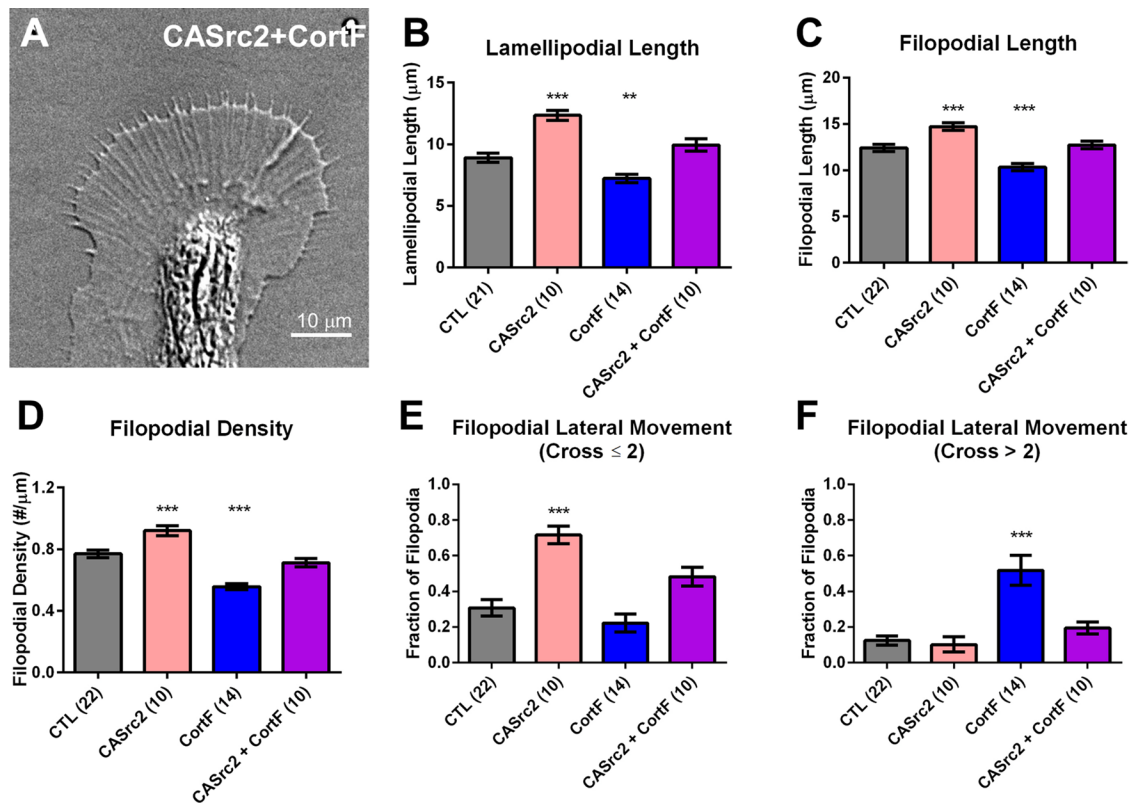
FIGURE 5: CortF abolishes CASrc2-induced lamellipodial and filopodial effects. (A) DIC live-cell image of *Aplysia* growth cone expressing CASrc2 and CortF. (B) Average lamellipodial length, (C) average filopodial length, (D) filopodial density, (E) fraction of filopodia undergoing small-scale lateral movement (cross two or fewer filopodia), and (F) fraction of filopodia undergoing large-scale lateral movement (cross more than two filopodia) in *Aplysia* growth cones expressing CASrc2, CortF, or both together compared with control (CTL) growth cones. Data are means ± SEM; numbers in parentheses are number of growth cones selected from at least three experiments. The *p* values are determined by one-way ANOVA with Dunnett's post hoc test, comparing each experimental group against a pooled control group. **$p < 0.01$, ***$p < 0.001$.

investigated which specific aspects of actin dynamics and organization are controlled by Src2 and cortactin. Actin assembly and retrograde flow are major determinants of the motile behavior of filopodia and lamellipodia in growth cones (Suter and Forscher, 2000; Lowery and Van Vactor, 2009). Using quantitative FSM, we tested whether Src2 and cortactin control rates of actin assembly and retrograde flow in filopodia (Figure 6) and lamellipodia (Supplemental Figure S5). Because actin filaments are highly organized in filopodia, individual actin speckles can be identified and tracked along filopodia using processed time-lapse montages (Figure 6, A and B, and Supplemental Videos S1–S5). None of our Src2 or cortactin manipulations significantly affected rates of actin assembly or retrograde flow during protrusion, retraction, or pausing phases (Figure 6, C–D″). Retrograde flow rates were on average 5.1 µm/min under all conditions, independent of protrusion, retraction, or pausing phases. Filopodial actin assembly rates averaged 7.1 µm/min during protrusion, 3.1 µm/min during retraction, and 5.1 µm/min during pausing phases. Comparison of these actin assembly and retrograde flow rates with filopodial protrusion/retraction rates (Figure 4, F and F″) indicates that the level of the actin assembly rate determines whether a filopodium protrudes, pauses, or retracts under these experimental conditions.

Because the actin meshwork close to the leading edge is very dense and not as highly organized as in filopodial actin bundles, measuring actin assembly rates in lamellipodia is challenging.

Therefore, we calculated the actin assembly rates in lamellipodia based on a model proposing that the leading-edge protrusion rate is determined by the rate of actin assembly minus the rate of retrograde flow (Suter and Forscher, 2000; Lowery and Van Vactor, 2009). We first tested this model on filopodia, for which we can experimentally determine protrusion/retraction, actin assembly, and retrograde flow rates, and found that filopodial protrusion/retraction rates had a strong linear correlation with the difference between actin assembly and retrograde flow rates (Supplemental Figure S5A, $R^2 = 0.98$). When this model was applied to lamellipodia, we found that, as in the case of filopodia, the rates of actin assembly and retrograde flow in lamellipodial veils were not significantly affected by up- or down-regulation of either Src2 or cortactin (Supplemental Figure S5, B–C″). In summary, our findings suggest that Src2 and cortactin regulate the length of filopodia and length of lamellipodia by controlling how much time growth cones spend in different states of actin assembly rather than directly controlling the rate of actin assembly itself.

Src2 and cortactin enhance the density of actin networks in lamellipodia

Because rates of actin assembly and retrograde flow were not significantly affected by Src2 or cortactin manipulation, we performed high-resolution SEM to investigate whether and how the structural organization of the actin cytoskeleton changes to result in the
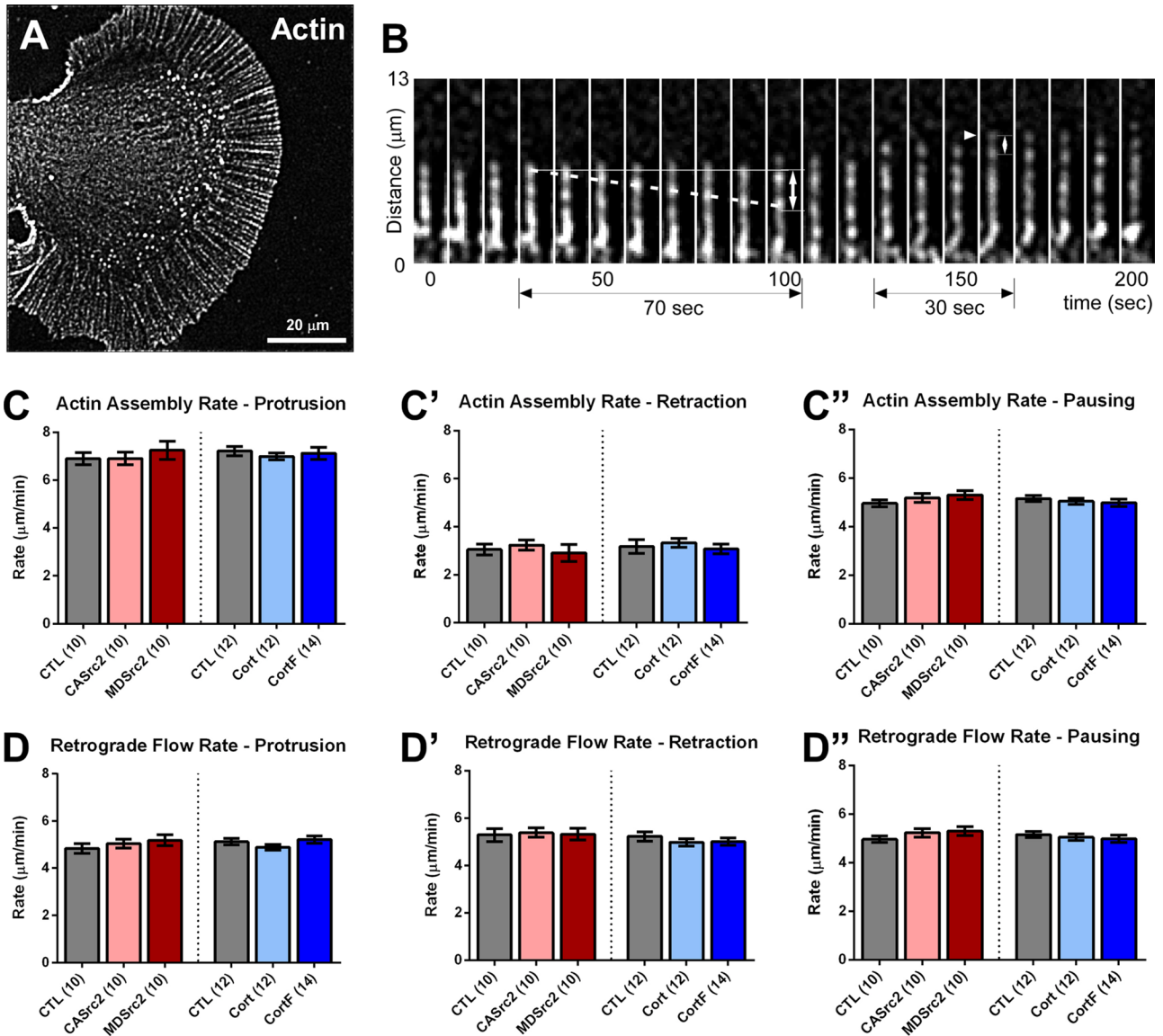
FIGURE 6: Actin dynamics in filopodia. (A) Processed actin FSM image of an *Aplysia* neuronal growth cone. (B) Representative time-lapse montage of a single filopodial actin bundle labeled with Alexa 568–G-actin. Internal speckles (dashed line) are tracked to calculate the retrograde flow rate. Similarly, the positions of newly added speckles (arrowhead) are determined to calculate the actin assembly rate. (C–C'') Actin assembly rates in filopodial tips in protrusion (C), retraction (C'), or pausing (C'') phases. (D–D'') Actin retrograde flow rates near filopodial tips in protrusion (D), retraction (D'), or pausing (D'') phases. Mean values ± SEM; numbers in parentheses are number of growth cones selected from at least three experiments. One-way ANOVA with Dunnett's post hoc test was separately performed for Src2 and cortactin conditions. No significant differences were determined between the different conditions.

lamellipodial and filopodial phenotypes that we observed after Src2 or cortactin up- or down-regulation (Figure 7). Control growth cones exhibited a dense actin network between regularly spaced, straight filopodia (Figure 7, A, D, and D'). Up-regulating Src2 or cortactin increased the density of actin meshwork and actin bundles (Figure 7, E, E', G, G', and I), whereas down-regulating Src2 activation or cortactin phosphorylation levels led to disorganized actin network and fewer, curved filopodial actin bundles (Figure 7, B, F, F', H, H', and J). We quantified the percentage of lamellipodia area that contains actin filaments but not actin bundles (referred to as "actin occupancy") as an indicator of actin network density (Figure 7, C and D'–H'). In control growth cones, the actin occupancy was 56%. This value was significantly increased to 70 and

75% in CASrc2- and cortactin-expressing growth cones, respectively, and reduced to 48 and 49% in MDSrc2- and CortF-expressing growth cones, respectively (Figure 7C). To confirm the importance of Src-mediated phosphorylation of cortactin in actin network formation, we found that CortF coexpression restored actin meshwork density in lamellipodia of CASrc2-expressing growth cones to levels similar to those in controls (Figure 7, C and I–K). Similar to what was found for the large-scale lateral movements of filopodia (Figure 5F), CASrc2 coexpression also reduced the effect of CortF on filopodial orientation, making them straighter, similar to control condition (Figure 7K). These results indicate that Src2 phosphorylation of cortactin promotes the formation of actin meshwork structures in lamellipodia and that both
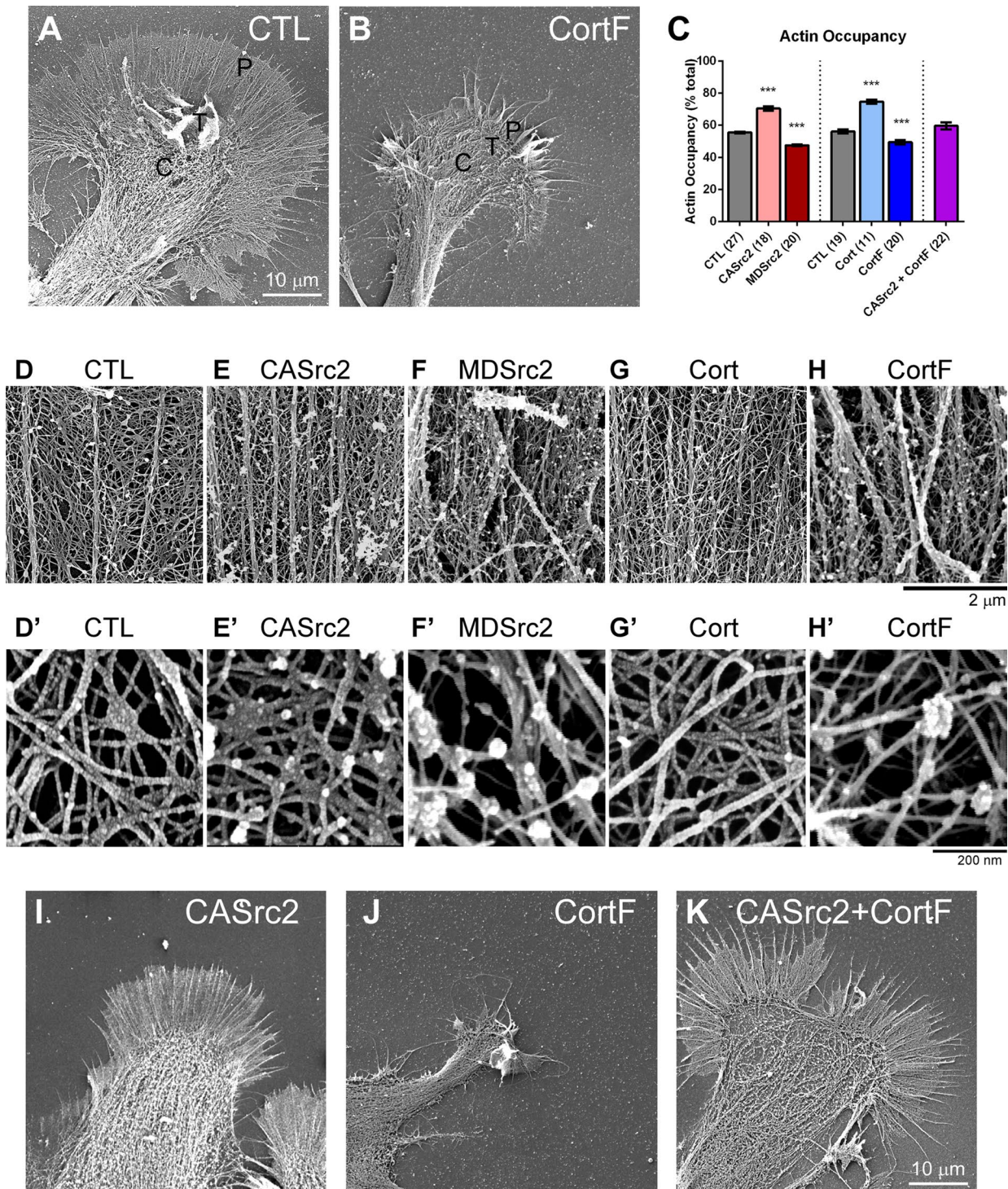
FIGURE 7: Src2 and cortactin increase the density of actin networks. (A) SEM image of control and (B) CortF-expressing growth cone. Control growth cones had regularly spaced filopodia with dense actin networks in between, whereas CortF-expressing growth cones showed fewer and curved filopodia, as well as lamellipodia that were retracted and contained disorganized actin networks of reduced density. (C) Quantification of actin filament occupancy as indicator of network density in lamellipodia with different Src and cortactin activity levels. CASrc2 and cortactin expression increased network density, whereas MDSrc2 and CortF expression had opposite effects. Mean values ± SEM; numbers in parentheses are number of growth cones selected from at least three experiments. One-way ANOVA with Dunnett's post hoc test separately performed for Src2 and cortactin groups; ***$p < 0.001$. (D–H) High- magnification SEM images of actin meshwork and F-actin bundles from control and CASrc2-, MDSrc2-, cortactin-, and CortF-expressing growth cones. (D′–H′) Higher-magnification SEM images of actin network in the lamellipodia leading edge of control and CASrc2-, MDSrc2-, cortactin-, and CortF-expressing growth cones. (I–K) Low-magnification SEM images of CASrc2-, CortF-, and CASrc2+CortF-expressing growth cones. Lamellipodial and filopodial orientation phenotypes induced by CortF were restored by CASrc2 coexpression. Scale bars as indicated.

Src2 and cortactin are critical for the proper orientation of F-actin bundles in filopodia.

Activated Src2 and cortactin partially colocalize in the growth cone periphery

Expression of individual Src2 and cortactin constructs and combinations strongly suggests that Src2 phosphorylation of cortactin controls lamellipodial and filopodial morphology and dynamics through regulation of the actin cytoskeleton such as by promoting actin network formation and filopodial formation and stability. CASrc2 coexpression was able to restore in CortF-expressing growth cones the straight, regularly spaced filopodia observed in controls (Figures 5F and 7K). A possible explanation of this result is that CASrc2 expression increases phosphorylation levels of endogenous cortactin, which compensates the negative effects caused by the exogenous cortactin phosphorylation mutant. Another possibility is that Src2 activity also controls the actin cytoskeleton via other pathways, which are independent of cortactin. To address this issue further, we performed superresolution imaging of activated Src2 (pSrc2), cortactin, and Arp2/3, a potential effector protein of cortactin, in neuronal growth cones (Figure 8). We previously showed by wide-field epifluorescence imaging that Src2, activated Src2, and cortactin partially colocalize with F-actin and with each other in the P domain of growth cones, particularly along the leading edge and filopodia (Decourt *et al.*, 2009).

Dual-color STORM imaging confirmed partial colocalization of activated Src2 and cortactin especially along filopodia and the leading edge of lamellipodia, as indicated in the overlays of the individual fluorophore localizations (Figure 8, A, B, D, and F), suggesting that these proteins may function at the same location in growth cone lamellipodia and filopodia. Of interest, cortactin was detected at relatively regular intervals of 0.47 ± 0.02 µm along filopodia (mean value ± SEM, 13 growth cones, 5 filopodia/growth cone; Figure 8, C and D), which is consistent with a periodic pattern of cortactin along growth cone filopodia developed by mouse cortical neurons and human SH-SY5Y neuroblastoma cells, although those occurred at larger intervals (Yamada *et al.*, 2013). The Arp2/3 complex is a major nucleator of actin filament assembly and branching in lamellipodia (Weed *et al.*, 2000; Uruno *et al.*, 2001; Weaver *et al.*, 2001, 2002). Arp3, a subunit of the Arp2/3 complex, showed a less dense labeling pattern than cortactin in lamellipodia and partially colocalized with cortactin along the leading edge of lamellipodia (Figure 8, E and F). The partial colocalization of these proteins is not surprising, considering their dynamic interactions. pSrc2/cortactin exhibits higher colocalization in filopodia than in lamellipodia (Figure 8F; unpaired *t* test, ****$p < 0.0001$). These superresolution localization data support our proposed function of Src2 and cortactin in facilitating actin branching in lamellipodia, as well as in formation and stabilization of filopodia; however, they also suggest that not all of Src2 and cortactin functions may require both proteins.

DISCUSSION
Src and cortactin regulate the persistence of lamellipodial protrusion in growth cones
This study provides new and comprehensive insights into the role of Src and cortactin in the regulation of growth cone lamellipodia and filopodia. Our results support a model in which Src and cortactin increase the persistence of lamellipodial protrusions by maintaining actin assembly at higher rates than retrograde flow for longer time periods (Figure 9, process 1). Up-regulation of Src2 activation state or cortactin protein levels resulted in longer lamellipodia than with control growth cones, whereas down-regulation of Src2 activation or cortactin phosphorylation state had opposite effects (Figure 1F and Supplemental Figure S3E). These changes in lamellipodial length can be explained by the increased lamellipodial protrusion persistence when up-regulating Src2 or cortactin and increased retraction persistence and frequency when down-regulating Src2 activation or cortactin phosphorylation (Figure 2).

To test the hypothesis that Src2 and cortactin regulate lamellipodial dynamics through actin cytoskeleton, we used high-resolution SEM to examine actin architecture and time-lapse FSM to investigate actin dynamics in growth cone lamellipodia. Our results showed that Src2 and cortactin enhanced actin meshwork density (Figure 7); however, neither Src2 nor cortactin strongly controlled the rates of lamellipodial protrusion or retraction, actin assembly, or retrograde flow (Figure 2 and Supplemental Figure S5), suggesting that Src2 and cortactin likely facilitate the process of actin nucleation, branch formation, and branch stabilization, as well as enabling actin assembly along the leading edge of growth cone lamellipodia, rather than directly regulating the rates of actin assembly or flow. On the basis of our data, we propose a model according to which Src2 and cortactin facilitate and/or stabilize Arp2/3 complex–dependent actin branches in lamellipodia, thereby enhancing lamellipodial protrusion (Figure 9, process 1). This model is in agreement with previous findings on Arp2/3 complex in growth cone lamellipodia (Korobova and Svitkina, 2008; Yang *et al.*, 2012; San Miguel-Ruiz and Letourneau, 2014) and on cortactin's regulatory role in Arp2/3-dependent actin branch formation and stabilization in nonneuronal cells (Weed *et al.*, 2000; Uruno *et al.*, 2001; Weaver *et al.*, 2001, 2002; Bryce *et al.*, 2005; Kempiak *et al.*, 2005; Kowalski *et al.*, 2005; Ammer and Weed, 2008; Cai *et al.*, 2008); however, Src was not specifically investigated in these studies. This hypothesis is supported by in vitro findings that actin assembly can be enhanced via Src, cortactin, N-WASP, Nck, and Arp2/3 (Tehrani *et al.*, 2007), as well as by studies on actin polymerization during invadopodium assembly of carcinoma cells (Oser *et al.*, 2010).

Previous studies in nonneuronal cells suggest that Src-mediated tyrosine phosphorylation of cortactin promotes cell migration and cancer metastasis (Huang *et al.*, 1998, 2003; Bourguignon *et al.*, 2001; Wang *et al.*, 2011). In agreement with these studies, our finding that only full-length cortactin, but not its triple tyrosine phosphorylation mutant, increased lamellipodial length, protrusion time, and actin network density (Figures 1, 2, and 7) implies a role of tyrosine-phosphorylated cortactin in actin organization of growth cone lamellipodia. Coexpression of CortF abolished the effects of CASrc2 expression (Figures 5B and 7C and Supplemental Figure S4, A–C), further suggesting that lamellipodial length, protrusion persistence, and actin network density are positively regulated by Src2-mediated phosphorylation of cortactin. Because we did not use a knockdown/overexpression rescue but instead used a constitutively active/dominant negative approach to dissect this signaling pathway, we believe that our results that CASrc2/CortF restored values to control levels are in support of the Src2/cortactin pathway, considering that the constructs shift the balance of total Src2 activity and cortactin phosphorylation state but do not eliminate endogenous proteins. However, on the basis of our analysis, we cannot exclude additional pathways from Src2 to lamellipodial actin network that do not require Src2-mediated tyrosine phosphorylation of cortactin. In fact, the partial colocalization of Src2, cortactin, and Arp3 in lamellipodia supports
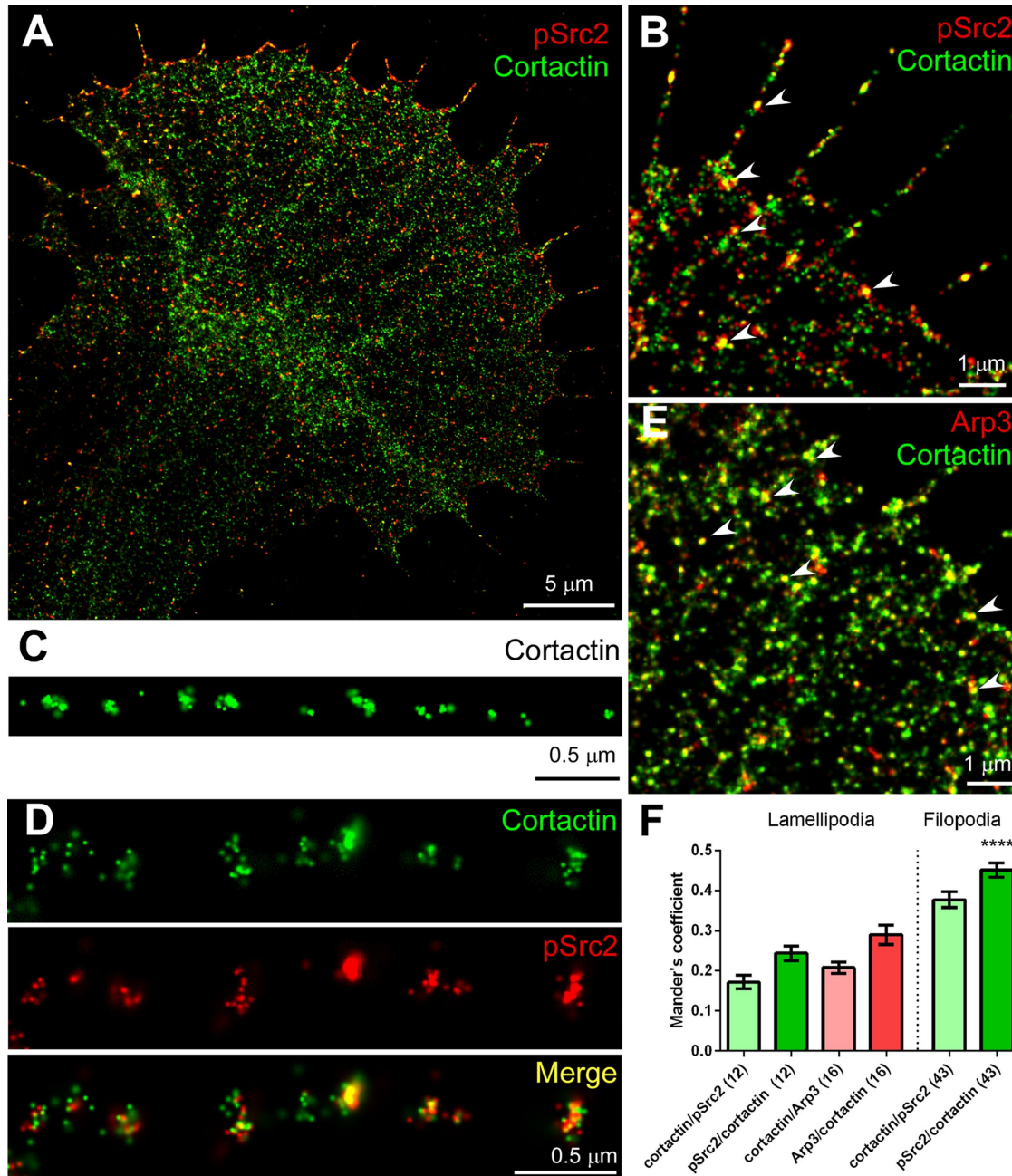
FIGURE 8: STORM imaging reveals partial colocalization of cortactin with activated Src2 and Arp2/3 complex. (A) STORM image depicting localization of activated Src2 (pSrc2; red) and cortactin (green) in an *Aplysia* growth cone. (B) Higher-magnification STORM image of activated Src2 and cortactin showing colocalization along filopodia and leading edge (arrowheads). (C) Clusters of cortactin labels were detected at regular intervals along a growth cone filopodium. (D) Another example of filopodium with double labeling of cortactin and activated Src2. Periodic pattern was detected in both channels, and stronger colocalization can be seen toward the tip of filopodium (right). (E) Partial colocalization of Arp3 (red) and cortactin (green) in growth cone lamellipodia and along filopodia (arrowheads). (F) Colocalization quantification of cortactin, activated Src2, or Arp2/3 complex in growth cone lamellipodia or along filopodia. Data are presented as Manders coefficient (mean values ± SEM). Numbers in parentheses refer to the number of growth cones analyzed in the case of lamellipodia and to the number of filopodia analyzed (13 cells). Cortactin/pSrc2 represents the ratio of cortactin signal overlapping with activated Src2 signal. pSrc2/cortactin represents the ratio of activated Src2 labeling overlapping with cortactin labeling. See *Materials and Methods* for details. Scale bars as indicated.

such an idea (Figure 8). In summary, our findings support a model in which Src2-mediated cortactin phosphorylation facilitates and/or stabilizes Arp2/3 complex–dependent actin branches in lamellipodia, thereby enhancing lamellipodial protrusion of growth cones (Figure 9, process 1).

Src and cortactin promote filopodia formation, stability, and elongation

Src (Robles *et al.*, 2005), cortactin (Yamada *et al.*, 2013), and Arp2/3 (Korobova and Svitkina, 2008; Norris *et al.*, 2009; Goncalves-Pimentel *et al.*, 2011; Spillane *et al.*, 2011; Yang *et al.*, 2012;
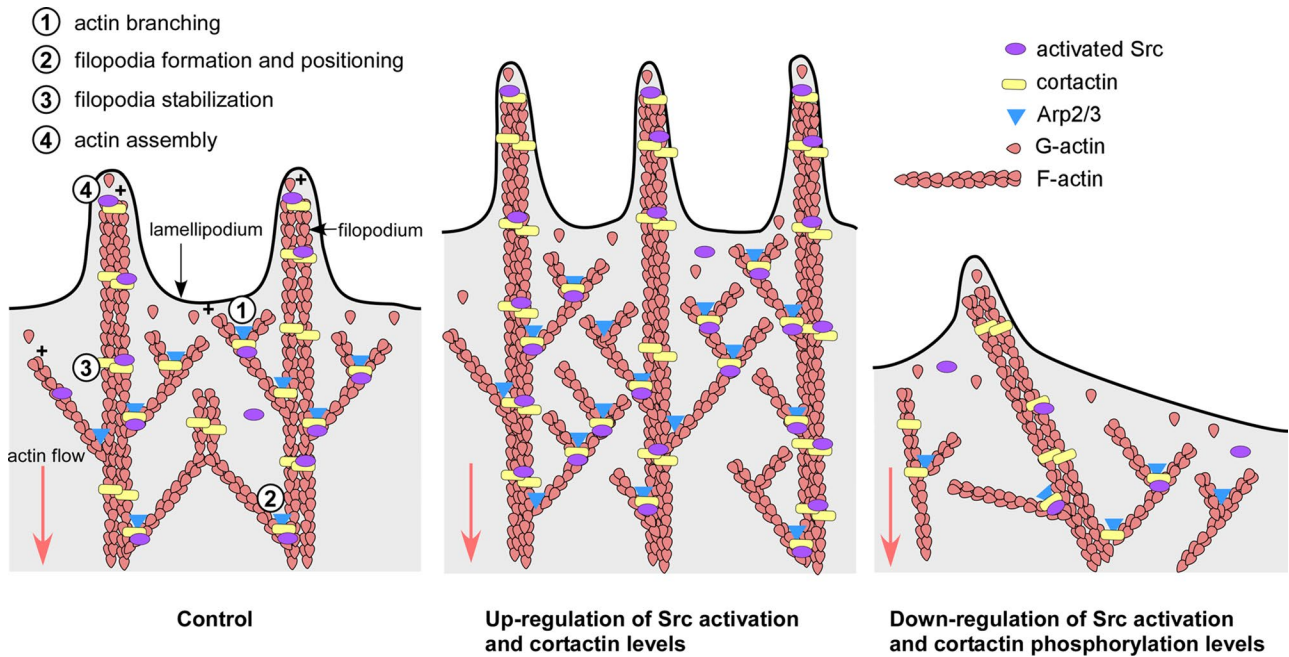
FIGURE 9: Model for Src/cortactin-mediated regulation of dynamics and morphology of growth cone lamellipodia and filopodia. Schematic depicting leading edge of lamellipodia and filopodia of neuronal growth cone in control condition (left), with up-regulated Src activation and cortactin levels (middle), and with down-regulated Src activation and cortactin tyrosine phosphorylation levels (right). 1) In lamellipodia, Src phosphorylation of cortactin facilitates Arp2/3 complex–dependent actin nucleation and branching, which results in lamellipodial protrusion. 2) Src and cortactin contribute to filopodia formation and positioning within the actin network by facilitating Arp2/3-mediated actin branch formation and stabilization. 3) In filopodia, Src phosphorylation of cortactin stabilizes bundles of actin filaments, resulting in straight filopodia. 4) Src and cortactin regulate the transition between different states of actin assembly at the plus end of filaments, thereby controlling persistence of protrusions. High rates of assembly occur during protrusion, whereas low rates of assembly occur during retraction. Up-regulation of Src activation and cortactin levels results in longer filopodia and lamellipodia, higher density of filopodia and actin network in lamellipodia, and more persistent actin-driven protrusions (middle). Down-regulation of Src activation and cortactin phosphorylation results in shorter filopodia and lamellipodia, reduced density of filopodia and actin network in lamellipodia, less persistent protrusions, and increased lateral movements of filopodia (right).

San Miguel-Ruiz and Letourneau, 2014) have been shown to promote filopodia formation in both growth cones and axons from different neuronal cell types. In agreement with these studies, we showed that Src2 and cortactin increased the density of filopodia (Figures 3H), which could be explained by increased formation of filopodia via Arp2/3-mediated actin branching (Figure 9, process 2) via a process referred to as convergent elongation (Yang and Svitkina, 2011) and/or by enhanced stability of filopodia (Figure 9, process 3), a process that likely involves dynamin instead of Arp2/3 (Yamada *et al.*, 2013). Coexpression of CortF and CASrc2 supports a role for Src2-dependent tyrosine phosphorylation in both of these processes (formation and stabilization; Figure 5D), although additional pathways cannot be excluded. In addition to Arp2/3, formins can also initiate growth cone filopodia (Goncalves-Pimentel *et al.*, 2011; Yang and Svitkina, 2011); however, much less is known about formin functions in growth cones than with Arp2/3.

We used MDSrc2 expression or PP2 treatment to reduce the Src2 activation state in growth cones. Knockdown of endogenous Src2 or cortactin was examined but not used because of low efficiency (unpublished data). The reduction of pSrc2 signal in MDSrc2-expressing cells suggests that MDSrc2 may compete with endogenous Src2 for Src activators. MDSrc2 expression, PP2 treatment, and CortF expression promoted large-scale lateral movements of filopodia and the occurrence of curved filopodia, whereas CASrc2 and cortactin expression increased the probability of small-scale lateral

movements of filopodia (Figure 3, I and J, Supplemental Figure S3F, and Supplemental Videos S1–S5). In addition, SEM revealed disorganized actin networks and bundles in growth cones expressing MDSrc2 or CortF (Figure 7). We speculate that both up- and down-regulation of Src and cortactin affect actin networks and bundles, resulting in an imbalance of actin-driven forces that controls the positioning of filopodia within lamellipodia compared with control conditions. These results indicate that Src and cortactin play a critical role in integrating filopodia within the lamellipodial actin network (Figure 9, process 2; most likely via Arp2/3), as well as in stabilizing actin bundles in filopodia (Figure 9, process 3; most likely via dynamin), consistent with recent studies proposing that cortactin and dynamin stabilize actin bundles in growth cone filopodia (Yamada *et al.*, 2013) and that cortactin stabilizes actin branches in nonneuronal cells (Weaver *et al.*, 2001; Cai *et al.*, 2008). The fact that CortF but not CASrc2 expression alone affected large-scale lateral movement of filopodia, whereas the combinatorial expression restored the phenotype to control levels, could suggest that CASrc2 acts through an additional pathway in this case. However, an alternative interpretation of these data is that under control conditions, most filopodia are stabilized by Src2-phosphorylated cortactin. This cannot be further enhanced by CASrc2 but can be reduced by CortF, which competes with phosphorylated cortactin on filopodia. In support of this role of Src2-mediated cortactin phosphorylation for stabilization of filopodial actin bundles, we observed a higher

level of Src2/cortactin colocalization in filopodia than in lamellipodia (Figure 8F).

As found for the length of lamellipodia, up-regulation of Src2 and cortactin increased the length of filopodia (Figure 4, A and B), which is consistent with previous findings on both proteins (Robles et al., 2005; Wu et al., 2008; Yamada et al., 2013). This elongation effect could be explained by the increased protrusion time and reduced retraction time and frequency when up-regulating Src2 and cortactin, as well as increased retraction time and frequency when down-regulating Src2 activity and cortactin phosphorylation levels (Figure 4, D, D', and E, and Supplemental Figure S4, D and E). Similar to lamellipodia, rates of filopodial protrusion/retraction, as well as of actin assembly and retrograde flow, were not significantly affected by these Src2 and cortactin manipulations (Figures 4, F and F', and 6, and Supplemental Figure S4F). These results suggest that Src2 and cortactin, most likely via Src2-dependent cortactin phosphorylation, stabilize actin filament bundles in growth cone filopodia, thereby increasing the persistence of protrusion (Figure 9, process 3). Furthermore, the increased persistence of actin assembly in filopodia when up-regulating Src2 or cortactin suggests that these proteins could also regulate the transition between different polymerization states at the barbed end of actin filaments, for example, by preventing the binding of capping protein (Figure 9, process 4).

In summary, the present work provides the first detailed and comprehensive quantitative analysis of how Src and cortactin together control actin organization and dynamics not only in growth cones but also in motile cells in general. Other potential Src substrates, including p190 Rho GTPase-activating protein (Brouns et al., 2001), N-WASP (Suetsugu et al., 2002), p21-activated kinase (Robles et al., 2005), and Nck (Tehrani et al., 2007; Ammer and Weed, 2008), are also likely involved in the regulation of the actin cytoskeleton. Insights gained from the present findings will be invaluable in future experiments investigating growth and guidance effects of cues that involve Src signaling.

MATERIALS AND METHODS
Src and cortactin constructs
The following untagged *Aplysia* Src2 and cortactin constructs were prepared in pRAT vector as described previously (Wu et al., 2008; Decourt et al., 2009): wild-type Src2, constitutively active Src2 (CASrc2), which is in the open and active conformation due to the tyrosine mutation in the regulatory C-terminus (Y518F); membrane localization–defective Src2 (MDSrc2), which is mutated in the N-terminal glycine residue (G2A) required for myristoylation and membrane targeting; and dominant negative Src2 (DNSrc2), which is a kinase-dead mutant in the open conformation (K286M Y518F). In addition, we prepared wild-type cortactin (Cort) and cortactin tyrosine phosphorylation–defective mutant (CortF, Y499F-Y505F-Y509F). These tyrosine phosphorylation sites were identified based on sequence comparisons with vertebrate cortactin homologues. Mutations were introduced using the QuikChange II site-directed mutagenesis kit (Agilent Technologies, Santa Clara, CA). We expressed untagged constructs to avoid any potential functional effects of fluorescent protein tags. All growth cones analyzed in the present study were assessed for Src2 or cortactin levels with immunostaining after time-lapse imaging, and only those growth cones with at least 50% higher protein levels than controls were included in the analysis.

Aplysia bag cell neuronal culture
Aplysia bag cell neurons were cultured in L15 medium (Invitrogen, Life Technologies, Grand Island, NY) supplemented with artificial seawater (L15-ASW: L15 plus 400 mM NaCl, 9 mM $CaCl_2$, 27 mM

$MgSO_4$, 28 mM $MgCl_2$, 4 mM L-glutamine, 50 µg/ml gentamicin, 5 mM 4-(2-hydroxyethyl)-1-piperazineethanesulfonic acid, pH 7.9) on coverslips coated with 20 µg/ml poly-L-lysine (70–150 kDa; Sigma-Aldrich, St. Louis, MO) as described previously (Suter, 2011).

mRNA expression in *Aplysia* neurons
mRNAs of *Aplysia* Src and cortactin constructs were prepared using the mMESSAGE mMACHINE T7 in vitro transcription kit (Ambion, Life Technologies, Grand Island, NY) and expressed by microinjection into *Aplysia* bag cell neurons typically 18–24 h after cell plating. mRNA, 3 mg/ml in 10 mM Tris, pH 8.0, 1 mM EDTA was heated at 65°C for 5 min, mixed with an equal volume of 3 mg/ml Alexa 568-G actin (Life Technologies) in G-buffer (2 mM Tris-HCl, 0.2 mM $CaCl_2$, 0.2 mM ATP, 0.5 mM dithiothreitol), and spun at 14,000 × g for 30 min at 4°C before microinjection. Microinjection was performed using the NP2 micromanipulator and FemtoJet microinjection system (Eppendorf, Hauppauge, NY). Reagent solution injection volumes were typically ~10–15% of cell volume. After microinjection, neurons were incubated in culture medium for 48 h before imaging.

Fluorescent speckle microscopy
FSM of actin dynamics was performed as previously described (Lee and Suter, 2008), using a Nikon TE2000 E2 Eclipse inverted microscope equipped with a 60×/1.4 numerical aperture (NA) oil immersion objective plus additional 1.5× magnification or a 100×/1.49 NA objective (Nikon, Melville, NY) and a Cascade II charge-coupled device camera (Photometrics, Tucson, AZ) controlled by MetaMorph 7.8 software (Molecular Devices, Sunnyvale CA). Fluorescent illumination was provided by an X-cite 120Q metal halide lamp (Excelitas Technologies, Waltham, MA) and appropriate single-bandpass filter sets (Chroma, Bellows Falls, VT). Live- cell imaging was performed at room temperature in ASW supplemented with 2 mg/ml bovine serum albumin (BSA), 1 mg/ml *l*-carnosine, and 0.25 mM vitamin E. Fluorescence images were taken at 10-s intervals for time periods of 15–20 min.

Analysis of protrusion and actin dynamics
MetaMorph 7.8 was used for image processing, montage, and kymograph preparation as previously described (Lee and Suter, 2008). We measured the length of lamellipodia as the distance between the T zone and the leading edge (Figure 1) and the length of filopodia as the distance between the T zone and filopodial tips (Figure 4A). Protrusion and retraction rates of filopodia or lamellipodia were determined by tracking filopodial tips or lamellipodial leading edge, respectively. Protrusion phases were defined by protrusion rates of ≥0.5 µm/min; retraction phases by retraction rates of ≥0.5 µm/min; and pausing phases by protrusion/retraction rates of <0.5 µm/min. Protrusion and retraction frequencies were determined as the frequency of entering into a protrusion and retraction phase, respectively, from any other phases. The percentage of time and the corresponding protrusion/retraction rates spent in each phase were quantified from 10–14 growth cones with 2–4 filopodia or lamellipodia regions. For analysis of filopodial actin dynamics, actin assembly rate was measured as the distance between the newest speckle close to the tip and the most recent tip speckle divided by the elapsed time, and retrograde flow rate was measured as the rate at which a speckle travels away from the filopodial tip. For analysis of lamellipodial actin dynamics, retrograde flow rate was determined by drawing a 1-pixel-wide line using the kymograph function in MetaMorph 7.8, and actin assembly rate was calculated by adding leading-edge protrusion and retrograde flow rate determined from actin kymographs.

Immunocytochemistry

Immunostaining was performed immediately after live-cell imaging to determine the expression levels of *Aplysia* Src and cortactin. Only growth cones expressing at least 50% more Src2/cortactin than controls were included in our functional analysis. Cultured cells were fixed with 3.7% formaldehyde in ASW plus 400 mM sucrose for 30 min at room temperature, followed by permeabilization with 0.05% saponin in fixative for 10 min (Wu *et al.*, 2008; Decourt *et al.*, 2009). Washing was performed in phosphate-buffered saline (PBS)/0.005% saponin. Blocking was carried out with 5% BSA (cortactin and Arp3 staining) or 10% horse serum (Src staining) in wash buffer for 30 min. Primary antibodies diluted in blocking solution were incubated for 1 h at room temperature: monoclonal anti-cortactin antibody 4F11 (Millipore, Billerica, MA) at 2 µg/ml; goat anti-Src2 antibody and rabbit anti–activated Src2 (pSrc2) antibody (Wu *et al.*, 2008) at 2.5 µg/ml; and rabbit anti-Arp3 antibody (Millipore) at 5 µg/ml. Corresponding Alexa 488–conjugated (for Src2) and 647–conjugated (for pSrc2, Arp3, or cortactin) secondary antibodies (Life Technologies) were sequentially incubated at 1 µg/ml in wash buffer for 30 min. After several washes, cells were observed by fluorescence microscopy in an antifading medium (20 mM *n*-propyl-gallate in PBS/80% glycerol, pH 8.5). Control experiments were conducted by omitting primary antibodies and resulted in very low background staining.

STORM imaging

All steps until secondary antibody incubation were carried out as for regular immunolabeling. For STORM imaging, the following three secondary antibodies were made by double labeling goat anti-mouse immunoglobulin G (IgG) and goat anti-rabbit IgG (Life Technologies) with reporter (Alexa Fluor 647–carboxylic acid succinimidyl ester; Life Technologies) and activator dyes (Cy2 reactive dye; Cy3 reactive dye; GE): goat anti-mouse IgG-AF647-Cy2, goat anti-mouse IgG-AF647-Cy3, and goat anti-rabbit IgG-AF647-Cy3. For all secondary antibodies, the ratio antibody:reporter:activator was ~1:3:5.5. After incubation with secondary antibodies for 30 min, samples were washed three times and postfixed with 4% formaldehyde in PBS/0.05% saponin for 5 min, washed again, and switched into imaging buffer (50 mM Tris-HCl, pH 8.0, 10 mM NaCl, 0.6 mg/ml glucose oxidase (Sigma-Aldrich), 34 µg/ml catalase (Roche, Indianapolis, IN), 10% (wt/vol) glucose, and 1% (vol/vol) 2-mercaptoethanol). Samples were imaged on a Nikon Ti-E–based N-STORM system for 20 min using 5–10% laser intensity for activation at 489 nm (Cy2) or 561 nm (Cy3) and 100% laser intensity for imaging at 647 nm. The STORM images represent a rendering of thousands of individual fluorophore localizations.

Colocalization analysis

Colocalization analysis of STORM images was performed using the JACoP plug-in in ImageJ (National Institutes of Health, Bethesda, MD). The Manders coefficient was chosen to represent the extent of overlap between red and green channels. Briefly, the coefficient for the red channel shows the ratio of summed intensities from pixels that have nonzero intensity in both red and green channels to the summed intensities from pixels in the red channel, and the coefficient for the green channel is calculated conversely. All coefficients were generated after thresholding the images from both channels. Analysis of colocalization in the P domain was performed by selecting the outmost one-fourth region of lamellipodia, and analysis of colocalization in filopodia was done by selecting the part of filopodia between leading edge of lamellipodia and filopodial tips.

Scanning electron microscopy

Aplysia neurons were live extracted as previously described (Decourt *et al.*, 2009) and then fixed with 2% glutaraldehyde in 0.1 M cacodylate buffer, pH 7.4, followed by 2% tannic acid and 0.1% uranyl acetate, each step for 20 min at room temperature with water washing in between. All reagents for SEM sample preparation were from Electron Microscopy Sciences (Hatfield, PA). Samples were dehydrated with an increasing ethanol concentration series before critical-point drying. Specimens were sputter-coated with platinum, and regions near lamellipodia leading edge were imaged with a FEI NOVA nanoSEM (FEI, Hillsboro, OR) in the Purdue Life Science Microscopy Facility at 5-kV voltage and 25,000–250,000× magnification. To analyze actin meshwork density, an intensity threshold was applied using ImageJ to distinguish actin filaments from open areas. Actin occupancy was determined as the percentage area occupied by actin filaments from 4–10 nonoverlapping regions using the analyze particle function in ImageJ. From 11 to 22 growth cones were analyzed for each condition.

Statistics

All histograms and statistical analyses were performed in GraphPad Prism (GraphPad Software, La Jolla, CA). The *p* values were determined by one-way analysis of variance (ANOVA) with Dunnett's post hoc tests. Statistical significance was defined as $p < 0.05$.

REFERENCES

Ammer AG, Weed SA (2008). Cortactin branches out: roles in regulating protrusive actin dynamics. Cell Motil Cytoskeleton 65, 687–707.

Bagrodia S, Taylor SJ, Shalloway D (1993). Myristylation is required for Tyr-527 dephosphorylation and activation of pp60c-src in mitosis. Mol Cell Biol 13, 1464–1470.

Bashaw GJ, Klein R (2010). Signaling from axon guidance receptors. Cold Spring Harb Perspect Biol 2, a001941.

Bourguignon LY, Zhu H, Shao L, Chen YW (2001). CD44 interaction with c-Src kinase promotes cortactin-mediated cytoskeleton function and hyaluronic acid-dependent ovarian tumor cell migration. J Biol Chem 276, 7327–7336.

Brouns MR, Matheson SF, Settleman J (2001). p190 RhoGAP is the principal Src substrate in brain and regulates axon outgrowth, guidance and fasciculation. Nat Cell Biol 3, 361–367.

Bryce NS, Clark ES, Leysath JL, Currie JD, Webb DJ, Weaver AM (2005). Cortactin promotes cell motility by enhancing lamellipodial persistence. Curr Biol 15, 1276–1285.

Cai L, Makhov AM, Schafer DA, Bear JE (2008). Coronin 1B antagonizes cortactin and remodels Arp2/3-containing actin branches in lamellipodia. Cell 134, 828–842.

Cheng Y, Leung S, Mangoura D (2000). Transient suppression of cortactin ectopically induces large telencephalic neurons towards a GABAergic phenotype. J Cell Sci 113, 3161–3172.

Conde C, Caceres A (2009). Microtubule assembly, organization and dynamics in axons and dendrites. Nat Rev Neurosci 10, 319–332.

Decourt B, Munnamalai V, Lee AC, Sanchez L, Suter DM (2009). Cortactin colocalizes with filopodial actin and accumulates at IgCAM adhesion sites in Aplysia growth cones. J Neurosci Res 87, 1057–1068.

Dent EW, Gupton SL, Gertler FB (2011). The growth cone cytoskeleton in axon outgrowth and guidance. Cold Spring Harb Perspect Biol 3, a001800.

Falk J, Bechara A, Fiore R, Nawabi H, Zhou H, Hoyo-Becerra C, Bozon M, Rougon G, Grumet M, Puschel AW, et al. (2005). Dual functional activity of semaphorin 3B is required for positioning the anterior commissure. Neuron 48, 63–75.

Gomez TM, Letourneau PC (2014). Actin dynamics in growth cone motility and navigation. J Neurochem 129, 221–234.

Goncalves-Pimentel C, Gombos R, Mihaly J, Sanchez-Soriano N, Prokop A (2011). Dissecting regulatory networks of filopodia formation in a Drosophila growth cone model. PLoS One 6, e18340.

Huang J, Asawa T, Takato T, Sakai R (2003). Cooperative roles of Fyn and cortactin in cell migration of metastatic murine melanoma. J Biol Chem 278, 48367–48376.

Huang C, Liu J, Haudenschild CC, Zhan X (1998). The role of tyrosine phosphorylation of cortactin in the locomotion of endothelial cells. J Biol Chem 273, 25770–25776.

Ignelzi MA Jr, Miller DR, Soriano P, Maness PF (1994). Impaired neurite outgrowth of src-minus cerebellar neurons on the cell adhesion molecule L1. Neuron 12, 873–884.

Itoh B, Hirose T, Takata N, Nishiwaki K, Koga M, Ohshima Y, Okada M (2005). SRC-1, a non-receptor type of protein tyrosine kinase, controls the direction of cell and growth cone migration in C. elegans. Development 132, 5161–5172.

Kao TJ, Palmesino E, Kania A (2009). SRC family kinases are required for limb trajectory selection by spinal motor axons. J Neurosci 29, 5690–5700.

Kempiak SJ, Yamaguchi H, Sarmiento C, Sidani M, Ghosh M, Eddy RJ, Desmarais V, Way M, Condeelis J, Segall JE (2005). A neural Wiskott-Aldrich Syndrome protein-mediated pathway for localized activation of actin polymerization that is regulated by cortactin. J Biol Chem 280, 5836–5842.

Knoll B, Drescher U (2004). Src family kinases are involved in EphA receptor-mediated retinal axon guidance. J Neurosci 24, 6248–6257.

Korobova F, Svitkina T (2008). Arp2/3 complex is important for filopodia formation, growth cone motility, and neuritogenesis in neuronal cells. Mol Biol Cell 19, 1561–1574.

Kotani T, Morone N, Yuasa S, Nada S, Okada M (2007). Constitutive activation of neuronal Src causes aberrant dendritic morphogenesis in mouse cerebellar Purkinje cells. Neurosci Res 57, 210–219.

Kowalski JR, Egile C, Gil S, Snapper SB, Li R, Thomas SM (2005). Cortactin regulates cell migration through activation of N-WASP. J Cell Sci 118, 79–87.

Kurklinsky S, Chen J, McNiven MA (2011). Growth cone morphology and spreading are regulated by a dynamin-cortactin complex at point contacts in hippocampal neurons. J Neurochem 117, 48–60.

Lee AC, Suter DM (2008). Quantitative analysis of microtubule dynamics during adhesion-mediated growth cone guidance. Dev Neurobiol 68, 1363–1377.

Letourneau PC, Ressler AH (1984). Inhibition of neurite initiation and growth by taxol. J Cell Biol 98, 1355–1362.

Lewis AK, Bridgman PC (1992). Nerve growth cone lamellipodia contain two populations of actin filaments that differ in organization and polarity. J Cell Biol 119, 1219–1243.

Li W, Lee J, Vikis HG, Lee SH, Liu G, Aurandt J, Shen TL, Fearon ER, Guan JL, Han M, et al. (2004). Activation of FAK and Src are receptor-proximal events required for netrin signaling. Nat Neurosci 7, 1213–1221.

Liu G, Beggs H, Jurgensen C, Park HT, Tang H, Gorski J, Jones KR, Reichardt LF, Wu J, Rao Y (2004). Netrin requires focal adhesion kinase and Src family kinases for axon outgrowth and attraction. Nat Neurosci 7, 1222–1232.

Lowery LA, Van Vactor D (2009). The trip of the tip: understanding the growth cone machinery. Nat Rev Mol Cell Biol 10, 332–343.

Marsh L, Letourneau PC (1984). Growth of neurites without filopodial or lamellipodial activity in the presence of cytochalasin B. J Cell Biol 99, 2041–2047.

Martin GS (2001). The hunting of the Src. Nat Rev Mol Cell Biol 2, 467–475.

Mezi S, Todi L, Orsi E, Angeloni A, Mancini P (2012). Involvement of the Src-cortactin pathway in migration induced by IGF-1 and EGF in human breast cancer cells. Int J Oncol 41, 2128–2138.

Mingorance-Le Meur A, O'Connor TP (2009). Neurite consolidation is an active process requiring constant repression of protrusive activity. EMBO J 28, 248–260.

Norris AD, Dyer JO, Lundquist EA (2009). The Arp2/3 complex, UNC-115/abLIM, and UNC-34/Enabled regulate axon guidance and growth cone filopodia formation in Caenorhabditis elegans. Neural Dev 4, 38.

Oser M, Mader CC, Gil-Henn H, Magalhaes M, Bravo-Cordero JJ, Koleske AJ, Condeelis J (2010). Specific tyrosine phosphorylation sites on cortactin regulate Nck1-dependent actin polymerization in invadopodia. J Cell Sci 123, 3662–3673.

Parsons SJ, Parsons JT (2004). Src family kinases, key regulators of signal transduction. Oncogene 23, 7906–7909.

Robles E, Woo S, Gomez TM (2005). Src-dependent tyrosine phosphorylation at the tips of growth cone filopodia promotes extension. J Neurosci 25, 7669–7681.

Sabry JH, O'Connor TP, Evans L, Toroian-Raymond A, Kirschner M, Bentley D (1991). Microtubule behavior during guidance of pioneer neuron growth cones in situ. J Cell Biol 115, 381–395.

San Miguel-Ruiz JE, Letourneau PC (2014). The role of Arp2/3 in growth cone actin dynamics and guidance is substrate dependent. J Neurosci 34, 5895–5908.

Spillane M, Ketschek A, Donnelly CJ, Pacheco A, Twiss JL, Gallo G (2012). Nerve growth factor-induced formation of axonal filopodia and collateral branches involves the intra-axonal synthesis of regulators of the actin-nucleating Arp2/3 complex. J Neurosci 32, 17671–17689.

Spillane M, Ketschek A, Jones SL, Korobova F, Marsick B, Lanier L, Svitkina T, Gallo G (2011). The actin nucleating Arp2/3 complex contributes to the formation of axonal filopodia and branches through the regulation of actin patch precursors to filopodia. Dev Neurobiol 71, 747–758.

Suetsugu S, Hattori M, Miki H, Tezuka T, Yamamoto T, Mikoshiba K, Takenawa T (2002). Sustained activation of N-WASP through phosphorylation is essential for neurite extension. Dev Cell 3, 645–658.

Suter DM (2011). Live cell imaging of neuronal growth cone motility and guidance in vitro. Methods Mol Biol 769, 65–86.

Suter DM, Forscher P (2000). Substrate-cytoskeletal coupling as a mechanism for the regulation of growth cone motility and guidance. J Neurobiol 44, 97–113.

Suter DM, Forscher P (2001). Transmission of growth cone traction force through apCAM-cytoskeletal linkages is regulated by Src family tyrosine kinase activity. J Cell Biol 155, 427–438.

Suter DM, Schaefer AW, Forscher P (2004). Microtubule dynamics are necessary for SRC family kinase-dependent growth cone steering. Curr Biol 14, 1194–1199.

Sutherland DJ, Pujic Z, Goodhill GJ (2014). Calcium signaling in axon guidance. Trends Neurosci 37, 424–432.

Tehrani S, Tomasevic N, Weed S, Sakowicz R, Cooper JA (2007). Src phosphorylation of cortactin enhances actin assembly. Proc Natl Acad Sci USA 104, 11933–11938.

Thomas SM, Brugge JS (1997). Cellular functions regulated by Src family kinases. Annu Rev Cell Dev Biol 13, 513–609.

Tojima T, Hines JH, Henley JR, Kamiguchi H (2011). Second messengers and membrane trafficking direct and organize growth cone steering. Nat Rev Neurosci 12, 191–203.

Uruno T, Liu J, Zhang P, Fan Y, Egile C, Li R, Mueller SC, Zhan X (2001). Activation of Arp2/3 complex-mediated actin polymerization by cortactin. Nat Cell Biol 3, 259–266.

Vitriol EA, Zheng JQ (2012). Growth cone travel in space and time: the cellular ensemble of cytoskeleton, adhesion, and membrane. Neuron 73, 1068–1081.

Wang W, Liu Y, Liao K (2011). Tyrosine phosphorylation of cortactin by the FAK-Src complex at focal adhesions regulates cell motility. BMC Cell Biol 12, 49.

Weaver AM, Heuser JE, Karginov AV, Lee WL, Parsons JT, Cooper JA (2002). Interaction of cortactin and N-WASp with Arp2/3 complex. Curr Biol 12, 1270–1278.

Weaver AM, Karginov AV, Kinley AW, Weed SA, Li Y, Parsons JT, Cooper JA (2001). Cortactin promotes and stabilizes Arp2/3-induced actin filament network formation. Curr Biol 11, 370–374.

Weed SA, Karginov AV, Schafer DA, Weaver AM, Kinley AW, Cooper JA, Parsons JT (2000). Cortactin localization to sites of actin assembly in

lamellipodia requires interactions with F-actin and the Arp2/3 complex. J Cell Biol 151, 29–40.

Wong EV, Kerner JA, Jay DG (2004). Convergent and divergent signaling mechanisms of growth cone collapse by ephrinA5 and slit2. J Neurobiol 59, 66–81.

Wu B, Decourt B, Zabidi MA, Wuethrich LT, Kim WH, Zhou Z, MacIsaac K, Suter DM (2008). Microtubule-mediated Src tyrosine kinase trafficking in neuronal growth cones. Mol Biol Cell 19, 4611–4627.

Yamada H, Abe T, Satoh A, Okazaki N, Tago S, Kobayashi K, Yoshida Y, Oda Y, Watanabe M, Tomizawa K, et al. (2013). Stabilization of actin bundles by a dynamin 1/cortactin ring complex is necessary for growth cone filopodia. J Neurosci 33, 4514–4526.

Yam PT, Langlois SD, Morin S, Charron F (2009). Sonic hedgehog guides axons through a noncanonical, Src-family-kinase-dependent signaling pathway. Neuron 62, 349–362.

Yang C, Svitkina T (2011). Filopodia initiation: focus on the Arp2/3 complex and formins. Cell Adh Migr 5, 402–408.

Yang Q, Zhang XF, Pollard TD, Forscher P (2012). Arp2/3 complex-dependent actin networks constrain myosin II function in driving retrograde actin flow. J Cell Biol 197, 939–956.